

Modelling how ribavirin improves interferon response rates in hepatitis C virus infection

Narendra M. Dixit¹, Jennifer E. Layden-Almer², Thomas J. Layden² & Alan S. Perelson¹

¹Theoretical Biology and Biophysics, Theoretical Division, Los Alamos National Laboratory, Los Alamos, New Mexico 87545, USA

²Department of Medicine, University of Illinois at Chicago, Chicago, Illinois 60612, USA

Nearly 200 million individuals worldwide are currently infected with hepatitis C virus (HCV)¹. Combination therapy with pegylated interferon and ribavirin, the latest treatment for HCV infection, elicits long-term responses in only about 50% of patients treated^{2–4}. No effective alternative treatments exist for non-responders⁵. Consequently, significant efforts are continuing to maximize response to combination therapy^{6,7}. However, rational therapy optimization is precluded by the poor understanding of the mechanism(s) of ribavirin action against HCV⁸. Ribavirin alone induces either a transient early decline or no decrease in HCV viral load^{9–12}, but in combination with interferon it significantly improves long-term response rates^{2–4,13–15}. Here we present a model of HCV dynamics in which, on the basis of growing evidence^{16–21}, we assume that ribavirin decreases HCV infectivity in an infected individual in a dose-dependent manner. The model quantitatively predicts long-term response rates to interferon monotherapy and combination therapy, fits observed patterns of HCV RNA decline in patients undergoing therapy, reconciles conflicting observations of the influence of ribavirin on HCV RNA decline, provides key insights into the mechanism of ribavirin action against HCV, and establishes a framework for rational therapy optimization.

Ribavirin, a purine analogue, is phosphorylated within cells and incorporated into the RNA of replicating virions, thereby increasing the mutation frequency and reducing the specific infectivity of new virions²¹. We therefore assume that ribavirin (alone or in combination with interferon) renders a fraction of newly produced virions non-infectious and write the following equations to describe HCV dynamics in an individual undergoing combination therapy:

$$\frac{dI}{dt} = \beta TV_1 - \delta I \tag{1}$$

$$\frac{dV_1}{dt} = (1 - \rho)(1 - \varepsilon)pI - cV_1 \tag{2}$$

$$\frac{dV_{NI}}{dt} = \rho(1 - \varepsilon)pI - cV_{NI} \tag{3}$$

Infectious HCV virions, V_1 , infect target cells, T , to create productively infected cells, I , at rate βTV_1 . In the absence of therapy, each productively infected cell releases new virions at rate p . Interferon lowers p by a factor $(1 - \varepsilon)$, where ε is the effectiveness of interferon^{22,23}. Of the virions released, we assume that ribavirin renders a fraction ρ non-infectious, giving rise to the population V_{NI} . We call ρ the effectiveness of ribavirin. Productively infected cells are lost with first-order rate constant δ . Free virions are cleared from plasma with first-order rate constant c . The measured viral load $V = V_1 + V_{NI}$.

We present in Fig. 1 viral load decay profiles obtained by the numerical integration of equations (1)–(3) for three values of the loss rate of productively infected cells, $\delta = 0.01 \text{ d}^{-1}$, 0.14 d^{-1} and 0.4 d^{-1} , spanning the range estimated^{22–24}. To mimic the slow accumulation of ribavirin in plasma, we let ribavirin effectiveness

$\rho = \rho_{\max}(1 - \exp(-t/t_a))$, with the accumulation timescale $t_a = 5.6 \text{ d}$ (ref. 25). Ribavirin effectiveness, ρ , thus increases from 0 at $t = 0$ to the asymptotic value, ρ_{\max} , in $t \approx 28 \text{ d}$. Models assuming constant interferon effectiveness, ε , have successfully predicted plasma HCV RNA decline in patients under interferon therapy^{22,23}.

With constant ε , we find that V exhibits a biphasic decay with a fast first phase that lasts 1–2 d from the onset of therapy and a slow second phase for the rest of the treatment period. Interestingly, when ε is high, ribavirin has negligible influence on viral load decay. Theoretically, after two months of therapy with $\varepsilon = 0.95$, the difference in V when $\rho_{\max} = 0$ and 1 is less than $0.1 \log$ (1 log corresponds to a 10-fold change in HCV RNA copies per ml) (Fig. 1a). However, the distribution of V into infectious and non-infectious compartments differs, such that for $\delta = 0.14 \text{ d}^{-1}$ nearly half the virions are non-infectious by day 20 when $\rho_{\max} = 0.5$ (Fig. 1). When ε is low, ribavirin has a noticeable effect on viral load decay. After two months with $\varepsilon = 0.5$, V decays 2 logs and 4 logs for $\rho_{\max} = 0$ and 1, respectively, for $\delta = 0.14 \text{ d}^{-1}$, and the difference increases with δ (Fig. 1b). Further, this difference arises almost entirely from the second-phase decay of V .

In the second phase, viral production and clearance are in pseudo-equilibrium²²; that is, $(1 - \rho)(1 - \varepsilon)pI \approx cV_1$ and $\rho(1 - \varepsilon)pI \approx cV_{NI}$, which yields (Supplementary Note S1)

$$V = (1 - \varepsilon)V_0 \exp[-\delta(\varepsilon + \rho - \varepsilon\rho)t] \tag{4}$$

where V_0 is the viral load at the onset of therapy. Thus, the second-phase slope under combination therapy is $\delta(\varepsilon + \rho - \varepsilon\rho)$. The difference between this slope and the slope under interferon monotherapy ($\rho = 0$) is $\Delta = \delta(\varepsilon + \rho - \varepsilon\rho) - \delta\varepsilon = \delta\rho(1 - \varepsilon)$. Because $\Delta \approx 0$ when $\varepsilon \approx 1$, ribavirin has a negligible effect on the second-phase slope when interferon effectiveness is high. (However, a fraction, ρ , of the virions are non-infectious because of ribavirin; Supplementary Note S2.) As ε decreases, Δ increases and ribavirin enhances the second-phase slope. Viral load decrease in the first phase is about εV_0 and is independent of ρ . Indeed, in a recent study with high-dose daily interferon, in which for white genotype-1-infected subjects the mean ε was estimated at about 0.98, ribavirin seemed to have no effect on first-phase or second-phase kinetics²³.

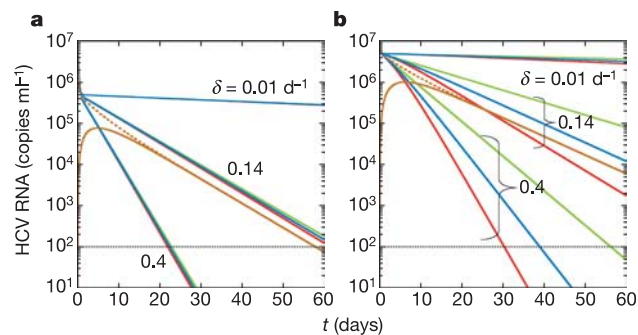


Figure 1 Theoretical viral load decay profiles. Equations (1)–(3) are solved for two values of interferon effectiveness, $\varepsilon = 0.95$ (a) and $\varepsilon = 0.5$ (b), with maximum ribavirin effectiveness of $\rho_{\max} = 1$ (red lines), 0.5 (blue lines) and 0 (green lines), a virion clearance rate of $c = 6.2 \text{ d}^{-1}$, an initial viral load of $V_0 = 10^7 \text{ ml}^{-1}$, and different values of the loss rate of productively infected cells, δ . We assume that the number density of target cells, T , remains constant at the pretreatment value $\delta c/\rho\beta$ (ref. 22). (Successful therapy should cause T to increase. We have performed calculations where we let T increase twofold over the duration of therapy and found a negligible influence on V .) Choosing a value for the virion production rate p is avoided because multiplication of equation (1) by p when $T = \delta c/\rho\beta$ enables consideration throughout of the composite variable Ip with initial value cV_0 . The distribution of viral load into infectious (V_1) (dashed orange lines) and non-infectious (V_{NI}) (solid orange lines) compartments is shown for $\delta = 0.14 \text{ d}^{-1}$ and $\rho_{\max} = 0.5$. The detection limit (dotted black line) is 100 copies ml^{-1} .

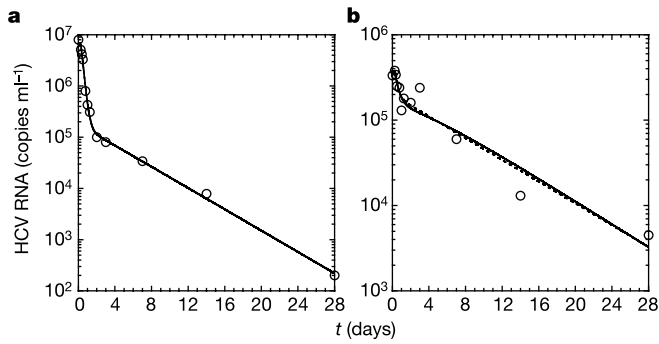


Figure 2 Comparison of theoretical viral load decay profiles with patient data. Best-fit model predictions (representative) of viral load decay with $\rho_{\max} = 1$ (solid lines) and $\rho_{\max} = 0$ (dashed lines) compared with data (symbols) from patients 18 (a) and 35 (b)²³. Parameters employed (Supplementary Table S1) were $V_0 = 8 \times 10^6 \text{ ml}^{-1}$, $c = 3.8 \text{ d}^{-1}$, $\delta = 0.24 \text{ d}^{-1}$, $\varepsilon = 0.982$ and $\tau = 4.3 \text{ h}$ for both $\rho_{\max} = 1$ and $\rho_{\max} = 0$ (a) and $V_0 = 3.6 \times 10^5 \text{ ml}^{-1}$, $c = 2.2 \text{ d}^{-1}$, $\delta = 0.16 \text{ d}^{-1}$, $\varepsilon = 0.6$ and $\tau = 6.2 \text{ h}$ for $\rho_{\max} = 1$, and $V_0 = 3.5 \times 10^5 \text{ ml}^{-1}$, $c = 3.1 \text{ d}^{-1}$, $\delta = 0.31 \text{ d}^{-1}$, $\varepsilon = 0.5$ and $\tau = 7.2 \text{ h}$ for $\rho_{\max} = 0$ (b). Note that the two fits overlap in a.

At the same time, another study found that ribavirin addition when $\varepsilon \approx 0.5$ had little influence on ε (obtained from the first phase) but increased the average value of δ (obtained from later phase(s)) twofold over interferon monotherapy²⁴. In a more recent study as well, ribavirin seemed to enhance the second-phase slope with standard thrice-a-week interferon in a dose-dependent manner but not with high-dose daily interferon¹². Our model thus reconciles these seemingly conflicting observations that ribavirin addition enhances viral load decline in some cases but not in others.

The above analysis rules out a major antiviral role for the immune modulatory effect of ribavirin, suggested as a key alternative mechanism of ribavirin action against HCV⁸. An immune modulatory effect would enhance the second-phase slope by increasing δ independently of ε . Thus, ribavirin would seem equally potent regardless of interferon effectiveness, contrary to the above observations^{12,23,24}.

We have applied our model to an analysis of viral load data obtained from 17 genotype-1-infected patients under combination therapy, who formed part of a larger study partly aimed at explaining the differences in the responses of white and African American patients to interferon-based therapy²³. Our model provides excellent fits to the data (Fig. 2, Supplementary Table S1 and Supplementary Fig. S1). We find that the best-fit parameter values obtained for patients with high interferon effectiveness are in close agreement with values obtained by models that ignore ribavirin action²³. This agreement is expected because with high interferon effectiveness ($\varepsilon \approx 1$) the addition of ribavirin has little influence on viral load decay. For African American patients in whom ε is much smaller than 1, the average value of δ , the loss rate of productively infected cells, obtained from the present fits is lower than that obtained with models that ignore ribavirin action²³. By

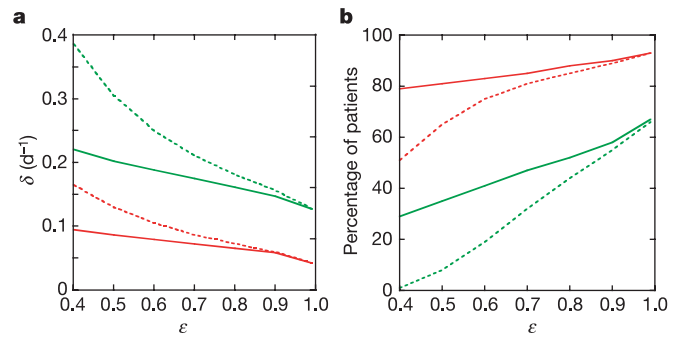


Figure 3 Model predictions of ETR and SVR. a, Minimum values of the loss rate of productively infected cells, δ , required for attaining ETR (red) and SVR (green). b, Fractions of patients treated for 24 weeks that would exhibit ETR (red) or SVR (green), respectively, with interferon monotherapy (dotted lines) or combination therapy assuming a ribavirin effectiveness of $\rho_{\max} = 0.5$ (solid lines), as functions of interferon effectiveness, ε (see Supplementary Table S2). Parameter values used are the initial viral load, $V_0 = 10^7$ copies ml^{-1} , virion clearance rate, $c = 9.5 \text{ d}^{-1}$, and the duration of the shoulder phase, $\tau = 0.3 \text{ d}$.

assuming a ribavirin effectiveness of $\rho = 0$, the latter models overestimate δ . Further, the average δ from present fits is similar for African American and white patients, indicating that the loss rate of productively infected cells might be race independent. Ribavirin, by lowering the infectivity of virions, diminishes the production rate of infected cells but does not influence their loss rate. That our model is able to distinguish between these subtle effects is remarkable and argues further against an immune modulatory role for ribavirin.

Two measures of the long-term outcome of therapy are commonly employed, namely end-of-treatment response (ETR) and sustained virological response (SVR), defined respectively as the plasma viral load below the assay detection limit at the end of treatment and the plasma viral load remaining below detection 24 weeks after the cessation of therapy. Ribavirin addition substantially increases both ETR and SVR, which we explain quantitatively with our model.

From equation (4), for given V_0 , ε and ρ , a minimum value of the loss rate of infected cells $\delta = \delta_{\text{ETR}}$ is required for V to reach the detection limit of 100 copies ml^{-1} at the end of treatment. A corresponding value, $\delta = \delta_{\text{SVR}}$, is required to reach the clearance limit, which we define as V less than one virion in the typical 15 l extracellular fluid volume (that is, 6×10^{-5} copies ml^{-1}) in humans. We assume that attaining the clearance limit results in SVR. For known ranges of V_0 , ε and ρ , we solve equations (1)–(3) to determine δ_{ETR} and δ_{SVR} (Fig. 3a, and Supplementary Table S2). Patients with $\delta \geq \delta_{\text{ETR}}$ will exhibit ETR and those with $\delta \geq \delta_{\text{SVR}}$ will exhibit SVR. δ varies significantly across patients and typically lies in the range 0.01–0.4 d^{-1} (refs 22–24). Here we assume that δ is normally distributed, with mean $\mu = 0.16 \text{ d}^{-1}$ and standard deviation $\sigma = 0.10 \text{ d}^{-1}$ deduced from fitting patient data (Supplementary Table S1). The probability that $\delta \geq \delta_{\text{ETR}}$ (or δ_{SVR}) then

Table 1 Comparison of model predictions and experimental observations

Duration of therapy		ETR (%)		SVR (%)	
		Interferon	Interferon + ribavirin	Interferon	Interferon + ribavirin
24 weeks	Observation	37–59	64–77	8–21	39–53
	Model prediction	65	80	*	35–41
48 weeks	Observation	31–68	71–94	17–24	53–72
	Observation (Peg-Interferon)	91	93–100	45	77
	Model prediction	88	93	56	76

The ETR and SVR are for interferon monotherapy and combination therapy with ribavirin (see refs 4, 13–15 and Supplementary Table S3).

*We employ observed SVR for 24 weeks of interferon monotherapy to set the interferon efficacy, ε , and thus do not predict it. SVR of 6–18% following 24 weeks of interferon monotherapy has been reported²⁴, which upon discounting for patients who did not complete the treatment course or were under reduced dose yields SVR of 8–21% (Supplementary Table S2). In our calculations, this range corresponds to $\varepsilon \sim 0.5$ –0.6 (Fig. 3), which is within the range for ε determined from viral dynamics studies²⁴. Addition of ribavirin when $\varepsilon \sim 0.5$ –0.6 yields an SVR prediction of 35–41% (Fig. 3, Supplementary Table S2) in agreement with the experimentally observed range of 39–53% (Supplementary Table S3). The remaining model predictions are all made with $\varepsilon \sim 0.5$.

yields the fraction of patients that would exhibit ETR (or SVR) (Fig. 3b and Supplementary Table S2). The best fits to the ETR and SVR data are obtained by assuming that 1,200 mg of ribavirin daily when given with interferon corresponds to $\rho_{\max} = 0.5$ (Supplementary Note S3). The difference in the ETR (SVR) values for $\rho_{\max} = 0$ and $\rho_{\max} = 0.5$ quantifies the enhancement in ETR (SVR) due to ribavirin addition.

Model predictions of ETR and SVR are in good agreement with experiments (Table 1). With $\varepsilon \approx 0.5$, obtained by fitting model predictions to SVR after 24 weeks of standard thrice-a-week interferon monotherapy, our model captures ETR and SVR after 24 weeks of standard interferon therapy and 48 weeks of pegylated interferon therapy with and without ribavirin. After 48 weeks of standard interferon therapy, however, model predictions overestimate ETR and SVR, indicating that $\varepsilon < 0.5$ for this case. Why ε seems to decrease from 24 to 48 weeks of standard interferon remains unknown. Perhaps the consistently higher incidence of side effects for 48 weeks of therapy³ compromises patient compliance. Greater compliance might be achieved with pegylated interferon, given the less frequent, weekly dosing, and might contribute to higher response rates (Supplementary Note S4). From all studies, the maximum enhancement in ETR or SVR by ribavirin addition is about 25–30% (Supplementary Table S3), as predicted by our model (Supplementary Table S2).

Our model thus provides a convincing picture of how ribavirin enhances HCV RNA decline and improves the long-term outcome of interferon-based therapy. Significant clinical implications follow. Because ribavirin influences the second and not the first phase of viral load decline, ε determined from the first phase underpredicts the long-term outcome of combination therapy²⁶. Because of enhanced second-phase decline, patients with slightly slower decays who might not achieve viral negativity under interferon monotherapy might become responders with combination therapy²⁷. In patients who achieve poor interferon effectiveness, for example some African American patients²³ or some patients infected with HCV genotype 1 (ref. 28), ribavirin addition should enhance second-phase decay²⁹ and improve ETR and SVR. For pegylated interferon α -2b administered weekly, during which ε might decrease significantly between doses³⁰, combination therapy might be particularly desirable. When ε is high, viral production is suppressed by interferon. As ε drops between doses, ribavirin can decrease the infectivity of new virions and prevent viral load resurgence¹².

By explicitly incorporating the anti-HCV activity of ribavirin, which extant models ignore^{22–24}, our model establishes a much-needed framework for the rational optimization of therapy. However, exploiting this framework requires an understanding of the possible synergy between ribavirin and interferon. This synergy is suggested by the observations that at the same ribavirin dosage, low ribavirin efficacy, $\rho_{\max} \ll 1$, accounts for the observed insignificant viral load decline under ribavirin monotherapy (Supplementary Note S5), but a much higher efficacy, $\rho_{\max} \approx 0.5$, explains long-term responses with combination therapy. We speculate on how this synergy might occur based on the modes of ribavirin and interferon action against HCV. Ribavirin is incorporated into the RNA of replicating genomes and gives rise to mutations, whose inherent frequency might be low. In the presence of interferon, viral production is diminished. The relative ribavirin concentration per replicating genome at membranous replication sites in an infected cell might then be elevated, which could increase the mutation frequency. At the same time, ribavirin lowers the intracellular guanosine triphosphate pools⁸, which might further increase the likelihood of ribavirin incorporation. When the mutation frequency is sufficiently high, replicating virions become non-infectious. Interferon could therefore provide the necessary impetus for the mutagenic activity of ribavirin to exert an observable antiviral effect against HCV. Although recent measurements *in vivo* indicate that mutation frequencies might not be significantly enhanced under

ribavirin monotherapy¹², mutation frequencies under combination therapy, which provide tests of this hypothesis, have not been measured. Nevertheless, our model applies so long as ribavirin decreases HCV infectivity, even if this occurs by mechanisms other than mutagenesis. □

Received 10 August; accepted 25 October 2004; doi:10.1038/nature03153.

1. World Health Organization, Hepatitis C—global prevalence (update). *World Health Org. Weekly Epidemiol. Rec.* **75**, 18–19 (2000).
2. National Institutes of Health, Consensus Statement on Management of Hepatitis C. *NIH Consens. State Sci. Statements* **19**, 1–46 (2002).
3. Manns, M. P. *et al.* Peginterferon α -2b plus ribavirin compared with interferon α -2b plus ribavirin for initial treatment of chronic hepatitis C: a randomised trial. *Lancet* **358**, 958–965 (2001).
4. Fried, M. W. *et al.* Peginterferon α -2a plus ribavirin for chronic hepatitis C virus infection. *N. Engl. J. Med.* **347**, 975–982 (2002).
5. Tan, S.-L., Pause, A., Shi, Y. & Sonenberg, N. Hepatitis C therapeutics: Current status and emerging strategies. *Nature Rev. Drug Discov.* **1**, 867–881 (2002).
6. Shiffman, M. L. *et al.* A randomized, controlled trial to determine whether continued ribavirin monotherapy in hepatitis C virus-infected patients who responded to interferon-ribavirin combination therapy will enhance sustained virologic response. *J. Infect. Dis.* **184**, 405–409 (2001).
7. Hoofnagle, J. H. *et al.* Maintenance therapy with ribavirin in patients with chronic hepatitis C who fail to respond to combination therapy with interferon alpha and ribavirin. *Hepatology* **38**, 66–74 (2003).
8. Lau, J. Y. N., Tam, R. C., Liang, T. J. & Hong, Z. Mechanism of action of ribavirin in the combination treatment of chronic HCV infection. *Hepatology* **35**, 1002–1009 (2002).
9. Dusheiko, G. *et al.* Ribavirin treatment for patients with chronic hepatitis C: results of a placebo-controlled study. *J. Hepatol.* **25**, 591–598 (1996).
10. Bodenheimer, H. C. *et al.* Tolerance and efficacy of oral ribavirin treatment of chronic hepatitis C: A multicenter trial. *Hepatology* **26**, 473–477 (1997).
11. Zoulim, F. *et al.* Ribavirin monotherapy in patients with chronic hepatitis C: a retrospective study of 95 patients. *J. Viral Hepat.* **5**, 193–198 (1998).
12. Pawlotsky, J.-M. *et al.* Antiviral action of ribavirin in chronic hepatitis C. *Gastroenterology* **126**, 703–714 (2004).
13. McHutchison, J. G. *et al.* Interferon α -2b alone or in combination with ribavirin as initial treatment for chronic hepatitis C. *N. Engl. J. Med.* **339**, 1485–1492 (1998).
14. Reichard, O. *et al.* Randomized, double-blind, placebo-controlled trial of interferon α -2b with and without ribavirin for chronic hepatitis C. *Lancet* **351**, 83–87 (1998).
15. Poynard, T. *et al.* Randomized trial of interferon α 2b plus ribavirin for 48 weeks or for 24 weeks versus interferon α 2b plus placebo for 48 weeks for treatment of chronic infection with hepatitis C virus. *Lancet* **352**, 1426–1432 (1998).
16. Lanford, R. E. *et al.* Antiviral effect and virus-host interactions in response to alpha interferon, gamma interferon, poly(I)-poly(C), tumor necrosis factor alpha, and ribavirin in hepatitis C virus subgenomic replicons. *J. Virol.* **77**, 1092–1104 (2003).
17. Contreras, A. M., Viral, R. N. A. *et al.* mutations are region specific and increased by ribavirin in a full-length hepatitis C virus replication system. *J. Virol.* **76**, 8505–8517 (2002).
18. Young, K.-C. *et al.* Identification of a ribavirin-resistant NS5B mutation of hepatitis C virus during ribavirin monotherapy. *Hepatology* **38**, 869–878 (2003).
19. Lanford, R. E. *et al.* Ribavirin induces error-prone replication of GB virus B in primary tamarin hepatocytes. *J. Virol.* **75**, 8074–8081 (2001).
20. Hong, Z. The role of ribavirin-induced mutagenesis in HCV therapy: A concept or a fact? *Hepatology* **38**, 807–810 (2003).
21. Crotty, S., Cameron, C. E. & Andino, R. RNA virus error catastrophe: Direct molecular test by using ribavirin. *Proc. Natl Acad. Sci. USA* **98**, 6895–6900 (2001).
22. Neumann, A. U. *et al.* Hepatitis C viral dynamics *in vivo* and the antiviral efficacy of interferon- α therapy. *Science* **282**, 103–107 (1998).
23. Layden-Almer, J. E., Ribeiro, R. M., Wiley, T., Perelson, A. S. & Layden, T. J. Viral dynamics and response differences in HCV-infected African American and white patients treated with IFN and ribavirin. *Hepatology* **37**, 1343–1350 (2003).
24. Herrmann, E., Lee, J.-H., Marison, G., Modi, M. & Zeuzem, S. Effect of ribavirin on hepatitis C viral kinetics in patients treated with pegylated interferon. *Hepatology* **37**, 1351–1358 (2003).
25. Glue, P. The clinical pharmacology of ribavirin. *Semin. Liv. Dis.* **19**, 17–24 (1999).
26. Steindl-Munda, P. *et al.* in *Abstracts 11th Int. Symp. Viral Hepatitis and Liver Dis.* 75–76 (2003).
27. Tsubota, A. *et al.* Viral dynamics and pharmacokinetics in combined interferon α -2b and ribavirin therapy for patients infected with hepatitis C virus of genotype 1b and high pretreatment viral load. *Intervirology* **45**, 33–42 (2002).
28. Neumann, A. U. *et al.* Differences in viral dynamics between genotypes 1 and 2 of hepatitis C virus. *J. Infect. Dis.* **182**, 28–35 (2000).
29. McHutchison, J. G. *et al.* The impact of interferon plus ribavirin on response to therapy in black patients with chronic hepatitis C. *Gastroenterology* **119**, 1317–1323 (2000).
30. Powers, K. A. *et al.* Modeling viral and drug kinetics: hepatitis C virus treatment with pegylated interferon α -2b. *Semin. Liv. Dis.* **23**, 13–18 (2003).

Supplementary Information accompanies the paper on www.nature.com/nature.

Acknowledgements We thank R. M. Ribeiro, J.-M. Pawlotsky, S. Zeuzem, X. Tong and B. Malcolm for helpful comments. Portions of this work were performed under the auspices of the US Department of Energy and supported by grants from the NIH, the University of Illinois and the Chicago VA.

Competing interests statement The authors declare that they have no competing financial interests.

Correspondence and requests for materials should be addressed to A.S.P. (asp@lanl.gov).